ACS APPLIED MATERIALS & INTERFACES

Research Article

www.acsami.org

Facile Synthesis of Few-Layer Graphene with a Controllable Thickness Using Rapid Thermal Annealing

Jae Hwan Chu,[†] Jinsung Kwak,[†] Tae-Yang Kwon,[†] Soon-Dong Park,[†] Heungseok Go,[‡] Sung Youb Kim,[†,§] Kibog Park,[‡] Seoktae Kang,[▽] and Soon-Yong Kwon*[,†,‡,§]

[†]School of Mechanical and Advanced Materials Engineering, Ulsan National Institute of Science and Technology, Ulsan 689-798, Republic of Korea

[‡]School of Electrical and Computer Engineering, Ulsan National Institute of Science and Technology, Ulsan 689-798, Republic of Korea

[§]Low Dimensional Carbon Materials Center, Ulsan National Institute of Science and Technology, Ulsan 689-798, Republic of Korea

[▽]Department of Civil Engineering, Kyung Hee University, Yongin 446-701, Republic of Korea

ABSTRACT: Few-layer graphene films with a controllable thickness were grown on a nickel surface by rapid thermal annealing (RTA) under vacuum. The instability of nickel films in air facilitates the spontaneous formation of ultrathin (<2−3 nm) carbon- and oxygen-containing compounds on a nickel surface; thus, the high-temperature annealing of the nickel samples without the introduction of intentional carbon-containing precursors results in the formation of graphene films. From annealing temperature and ambient studies during RTA, it was found that the evaporation of oxygen atoms from the surface is the dominant factor affecting the formation of graphene films. The thickness of the graphene layers is strongly dependent on the RTA temperature and time, and the resulting films have a limited thickness (<2 nm), even for an extended RTA time. The transferred films have a low sheet resistance of ∼0.9 ± 0.4 kΩ/sq, with ∼94% ± 2% optical transparency, making them useful for applications as flexible transparent conductors.

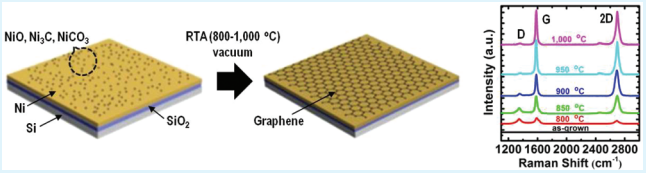

KEYWORDS: *graphene, rapid thermal annealing (RTA), few-layer, nickel, crystallization, transparent conductor*

1. INTRODUCTION

Graphene, which is a two-dimensional (2D) crystalline sheet of carbon atoms arranged in a honeycomb lattice, has emerged as a material with distinctive physical properties, such as ultrathin geometry,[1,2] quantum electronic transport,[2−4] tunable bandgap,[5,6] excellent thermal conductivity,[7] and high mechanical strength.[8] Since the discovery of the first isolated graphene, which was prepared via the mechanical exfoliation of graphite with small sizes of the order of micrometers,[1] graphene has been prepared via wet chemical synthesis,[9−13] thermal decomposition of silicon carbide,[14,15] surface precipitation process of carbon in some transition metals,[16−18] but it has been difficult to produce uniformly on large areas. Today, chemical vapor deposition (CVD) of hydrocarbon gases has been demonstrated as an attractive method to synthesize large-area graphene layers,[19−23] and the quality of the produced graphene is approaching industrially useful specifications.[24] However, special care should be taken to precisely control the resulting graphene layers in CVD, because of its sensitivity to various process parameters, making it difficult to apply the technology to a wider variety of potential feedstocks. Therefore, a facile synthesis to grow graphene layers with high controllability will have great advantages for scalable practical applications.

In order to simplify and create efficiency in graphene synthesis, the growth of graphene from solid carbon sources atop metal catalysts by the thermal annealing process has been discussed by several groups.[25−28] Recently, Pollard et al. reported the large-area, monolayer graphene synthesis using the very simple process of annealing nickel thin films led the process into converting trace amounts of unintentionally introduced carbon into graphene monolayers.[29] The process resulted in films with a higher monolayer fraction than alternative approaches to graphene growth on nickel, demonstrating that monolayer graphene can be simply grown with no need to deposit solid carbon sources. However, the study on the growth mechanism, the controllability in graphene thickness, and the detailed structural and optoelectronic properties in the resulting graphene films have not been reported yet, which will be of particular interest to explore for the practical application of graphene.

In this study, we report the growth of few-layer, large-area graphene films using rapid thermal annealing (RTA) without the use of intentional carbon-containing precursors and show that the resulting films have comparable structural and optoelectronic qualities to existing graphene materials grown on nickel via the CVD method. It was found that the instability of nickel films grown in commercial thin film evaporators and

Received: January 3, 2012
Accepted: March 7, 2012
Published: March 7, 2012

 © 2012 American Chemical Society dx.doi.org/10.1021/am3000177 | *ACS Appl. Mater. Interfaces* 2012, 4, 1777−1782

passed through atmosphere for a typical period of a few days facilitates the spontaneous formation of ultrathin (less than ~2−3 nm) carbon- and oxygen-containing compounds, such as NiO, Ni_3C, and $NiCO_3$ on a nickel surface. After the RTA process at a temperature as low as 800 °C or as high as 1000 °C (tested limit) under vacuum (~10^{-3} Torr), few-layer graphene films were formed on a nickel surface and the thickness of the resulting graphene layers is strongly dependent on the RTA temperature and time.

2. EXPERIMENTAL SECTION

2.1. Materials. We used nickel films with a thickness of ~100 nm deposited on a SiO_2(300 nm)/Si(100) wafer as substrates. The nickel films were deposited in several commercial evaporators (a base pressure of ~10^{-6}−10^{-7} Torr) with solid Ni (99.99% purity) as the source and stored under atmosphere for a typical period of a few days. The samples were then annealed at temperatures ranging from 800 °C to 1000 °C for 0.5−4 min, using an RTA system in various ambient environments.

2.2. X-ray Photoelectron Spectroscopy (XPS) Characterization. To measure the elemental composition, empirical formula, and chemical state of intrinsic impurities existing in Ni films before and after RTA, the XPS investigations were done on a K-alpha spectrometer (Thermo Fisher) using Al Kα nonmonochromatic X-ray excitation at a power of 72 W, with an analysis area ~0.4 mm in diameter and a pass energy of 50 eV for electron analysis.

A depth profile of the Ni films was obtained by combining a sequence of ion gun etch cycles interleaved with XPS measurements from the current surface. Each ion gun etch cycle exposes a new surface and the XPS spectra provide the means of analyzing the composition of these surfaces. For sputter depth profiling in this study, Ar^+ ions of 1 keV energy at a scan size of 2 mm × 2 mm and a sputter interval of 5 or 50 s were used, which resulted in a typical sputter rate of 0.215 nm/s for Ni films.

2.3. Raman Spectroscopy. Following the RTA process, the presence of graphene layers was confirmed by Raman spectroscopy, which is a fast and nondestructive method for the characterization of carbons.[30] The Raman spectra were carried out with a WiTec alpha 300R M-Raman system with 532 nm (2.33 eV) excitation. The laser spot size, when focused, was ~500 nm in diameter with a 50× optical lens. The Raman spectra from every spot of the sample were recorded, and data analysis was conducted using WiTec Project software.

2.4. Transmission Line Model (TLM) Measurement. The sheet resistance of graphene layers was measured using transmission line model (TLM) measurement, which is the way to measure the Ohmic contact resistance and the sheet resistance of the graphene layer precisely.[31−33] After transferring graphene layers onto a SiO_2(300 nm)/Si substrate, the graphene layers were patterned to a size of 150 μm × 1150 μm, with a Cr(10 nm)/Au(60 nm) bilayer as ohmic contacts. The distances between each 100 μm × 200 μm contact on the TLM structure were 50, 100, 200, and 300 μm. After the total resistance of the TLM structure was measured as a function of distance, we extracted a sheet resistance value of graphene from the slope.

3. RESULTS AND DISCUSSION

Figure 1 schematically illustrates our process for the growth of graphene layers on a nickel surface using RTA. We demonstrate the applicability of this method using nickel films as substrates. A key question here is how graphene can be derived from nickel films without the use of intentional carbon-containing precursors and it is also of interest to know if we can tune the structural and optoelectronic properties of the resulting graphene films using this method. As a first step, we have done XPS characterizations on nickel films to determine the source of carbon.

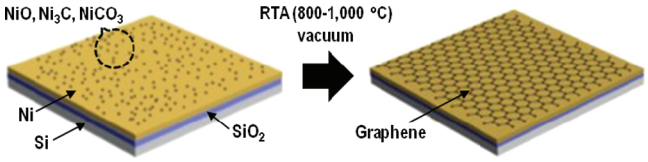

Figure 1. Schematic illustration for graphene growth with no necessity of depositing solid carbon sources on a Ni surface using RTA.

3.1. The Presence of Ultrathin Compounds on a Nickel Surface. A typical XPS concentration-depth profile of Ni films and the set of XPS spectra corresponding to the C 1s, O 1s, and Ni $2p_{3/2}$ peaks from a depth profile experiment are presented in Figure 2. One of the most important features of XPS is that the core level energy is dependent on the chemical state of the atom.[34−39] Changes in the local charge and potential of an atom cause shifts in core-level binding energies, so we can identify (i) the number and type of surrounding atoms, (ii) the electronegativity of atoms, and (iii) the oxidation state from the binding energy. We have consistently observed the presence of carbon atoms (~27% ± 3%) and oxygen atoms (~38% ± 1%) only at the surface of Ni film, as shown in Figure 2a, and it is found that the impurities coexist as compounds in the forms of NiO,[34−36] Ni_3C,[37,38] and $NiCO_3$[37,39] from the binding energy of each peak (see Figures 2b−d). This phenomenon has been observed, regardless of the thickness of Ni films deposited on a SiO_2(300 nm)/Si(100) substrate as well as types of evaporators, suggesting that trace amounts of unintentionally introduced carbon and oxygen atoms after Ni deposition may be converted into stable compounds on a catalytic Ni surface.

3.2. The RTA Process of Nickel Samples in Various Ambient. The samples were then annealed at temperatures ranging from 800 °C to 1000 °C for 0.5−4 min, using an RTA system under vacuum (~10^{-3} Torr) or in inert gas (Ar, N_2) in an ambient (~0.2−2.0 Torr) atmosphere. After the RTA process, few-layer graphene films are formed on a nickel surface under vacuum at all investigated temperature ranges, whereas no graphene forms when inert gases are introduced during the RTA process, regardless of the investigated temperatures and inert gas flow rates.

Figure 3a shows the results of Raman spectra of the nickel film covered by ultrathin carbon- and oxygen-containing compounds before RTA and the resulting graphene film on a nickel surface after RTA at temperatures in the range of 800−1000 °C for 0.5 min under vacuum. After the vacuum-RTA process, the Raman spectra show three primary features: a D band at ~1351 cm^{-1}, a G band at ~1584 cm^{-1}, and a 2D band at ~2689 cm^{-1}, all of which are expected peak positions for graphene.[19−24] From the Raman spectra of graphene layers grown after the RTA process at 850−1000 °C, we obtain (i) a ratio of G-to-2D peak intensities (I_G/I_{2D}) of ~0.85−1.1 and (ii) a full width at half maximum (FWHM) value of ~42−56 cm^{-1} for the 2D band, and (iii) a ratio of D-to-G peak intensities (I_D/I_G) of ~0.06−0.2, indicating few-layer graphene sheets with a relatively low defect density, which are similar to the previous reported graphene sheets grown by CVD on Ni substrates.[19,20] To check the crystallinity, the synthesized graphene film has been transferred onto a transmission electron microscopy (TEM) grid and the well-defined diffraction spots in the selected-area electron diffraction patterns confirm the crystalline structure of the graphene with a 6-fold symmetry (not shown here). Specifically, the Raman spectrum of graphene

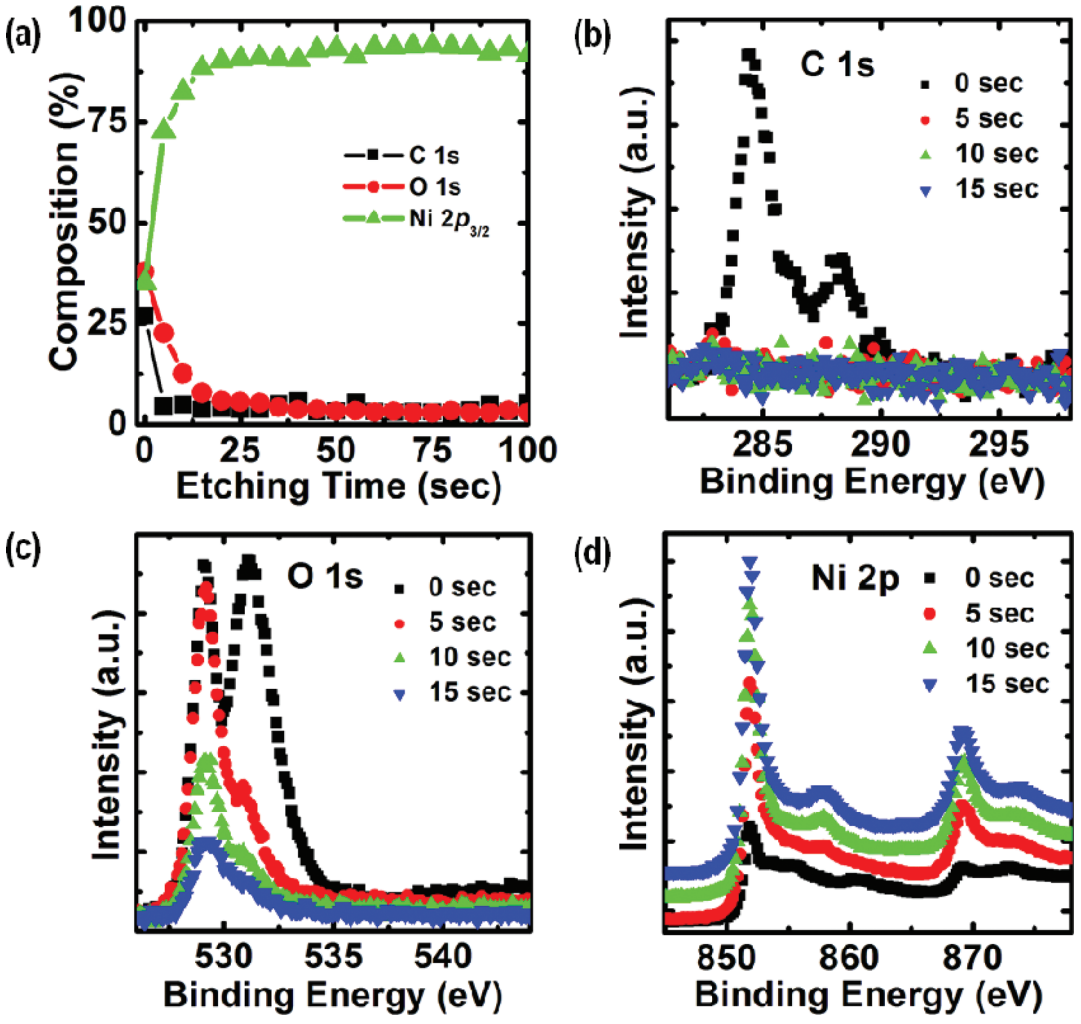

Figure 2. (a) Representative XPS concentration-depth profile of Ni films and (b–d) the set of XPS spectra corresponding to the C 1s, O 1s, and Ni $2p_{3/2}$ peaks from a depth profile experiment, showing the presence of ultrathin (less than ~2–3 nm) carbon- and oxygen-containing compounds such as NiO (853.8 eV for Ni $2p_{3/2}$, 529.7 eV for O 1s), Ni_3C (852.9 eV for Ni $2p_{3/2}$, 283.9 eV for C 1s) and $NiCO_3$ (854.7 eV for Ni $2p_{3/2}$, 531.3 eV for O 1s, 288.4 eV for C 1s) on a nickel surface.

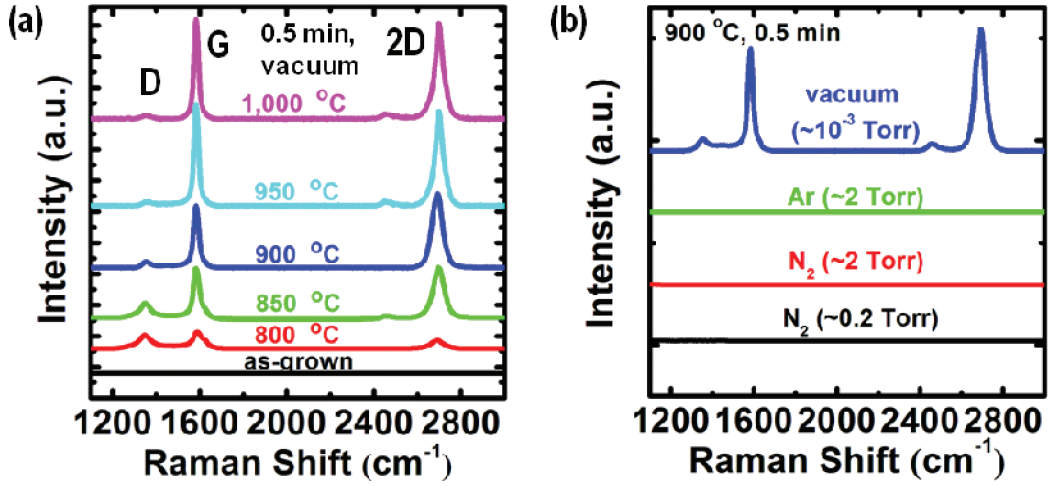

Figure 3. (a) Raman spectra of Ni films before and after the vacuum-RTA process at temperatures in the range of 800–1000 °C for 0.5 min. Graphene forms after the RTA process at all investigated temperature ranges, but the layer grown at 800 °C shows a high-intensity D peak. (b) Typical Raman spectra of resulting layers on Ni films after the RTA process at 900 °C for 0.5 min in a different ambient environment. Graphene forms only under vacuum in all investigated temperatures and ambient gas flow rates, indicating that the presence of the inert gas atmosphere prohibits the formation of graphene layers on Ni films.

dx.doi.org/10.1021/am3000177 | ACS Appl. Mater. Interfaces 2012, 4, 1777–1782

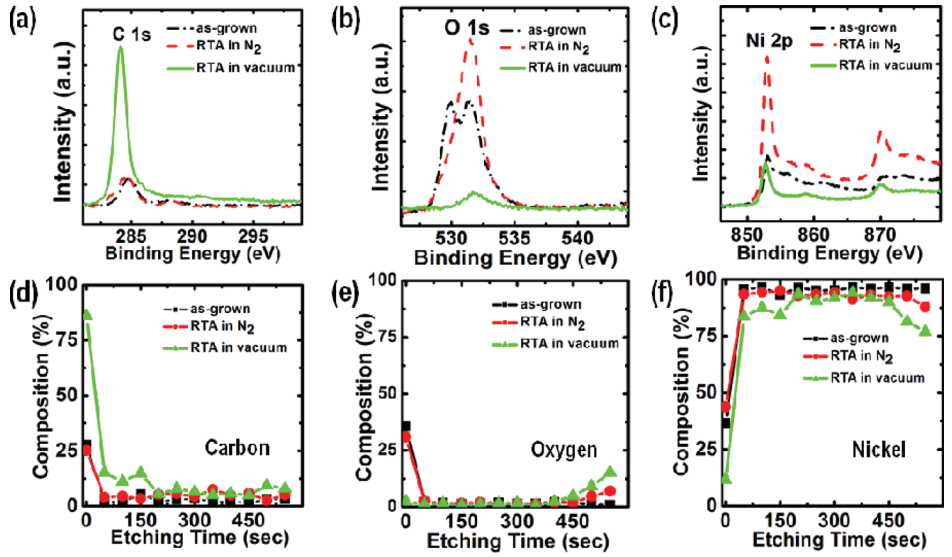

Figure 4. (a–c) Representative XPS concentration profile at the Ni surface and (d–f) the set of XPS spectra corresponding to the C 1s, O 1s, and Ni $2p_{3/2}$ peaks from a concentration-depth profile experiment of Ni films, depending on the RTA process in an ambient environment at 900 °C for 1 min.

layer obtained after the RTA process at 800 °C for 0.5 min shows a high-intensity D band; however, the value of I_D/I_G significantly drops to less than ~0.1 for an extended RTA time at 4 min (not shown here), suggesting that carbon atom rearrangement occurs and most of the topological defects are self-healed on a catalytic nickel surface at an extended annealing time under vacuum.

In stark contrast to the large-area graphene formation resulting from the vacuum-RTA process, the Raman spectra do not exhibit any carbon-related characteristics over a range of 1000–3000 cm^{-1} after the RTA process in an inert-gas ambient atmosphere, such as Ar or N_2, as shown in Figure 3b. From the XPS data in Figure 4, it is clear that the nickel surface undergoes considerable compositional changes only under vacuum and most oxygen atoms disappear after the vacuum-RTA process, possibly desorbing from the surface. It is noted that no significant change in oxygen concentration in Ni films is observed after an inert gas-RTA but the peak shift of O 1s XPS spectrum suggests that the main phase of oxygen-containing compounds on the Ni surface transforms to $NiCO_3$ (see Figure 4b). It is expected that the transformation of NiO to $NiCO_3$ would easily occur in the presence of carbon atoms on a nickel surface by considering the large difference in the heat formation of NiO (244.3 kcal/mol),[40] compared with $NiCO_3$ (713.4 kcal/mol).[41]

3.3. Growth Mechanism. We interpret the graphene growth mechanism as follows. The formation of graphene layers is observed after the vacuum-RTA process at temperatures in the range of 800–1000 °C, indicating that the formation of graphene on a nickel surface is thermally activated. Graphene formation at high temperatures over 460 °C is the result of nickel-catalyzed crystallization of solid carbon sources,[19,20,33] along with oxygen evaporation from the substrate under vacuum. For a given temperature, the presence of a high pressure of Ar or N_2 leads to a much-reduced oxygen evaporation rate because the dense cloud of inert gas molecules hinders the transport of oxygen atoms away from the nickel surface, as pointed out by Langmuir[42] and Fonda.[43] This hypothesis is supported by the fact that there is no significant change in elemental compositions of carbon and oxygen atoms on the Ni surface after an inert gas-RTA process, as shown in Figures 4d and 4e. Ultimately, in the presence of the inert gas atmosphere, a drastic reduction of the overall oxygen sublimation rate on the nickel surface results in no significant change in carbon and oxygen concentrations; however, the high substrate temperature during RTA facilitates the spontaneous transformation of the residual NiO into a stable phase of $NiCO_3$ in the presence of carbon atoms on the catalytic nickel surface.

3.4. Control of Graphene Thickness. In our process, the RTA temperature and time are critical for the thickness of the resulting graphene films grown under vacuum. After growing graphene layers on a Ni surface, ~1–2 μm-thick poly(methyl methacrylate) (PMMA) films were further spin-coated on the graphene layers for an effective transfer process. The PMMA/graphene layers were released from the Ni films by etching in a $FeCl_3$ solution (Figure 5a) and then transferred onto SiO_2 (300 nm)/Si or quartz substrates for further evaluation. The coated PMMA layers can be easily etched away using acetone, leaving behind the graphene films on the desired substrate. The existence of graphene on the transferred SiO_2 surface was confirmed by Raman spectroscopy, as shown in Figure 5b, and atomic force microscopy (AFM) was utilized to investigate the thickness of transferred graphene layers systematically, as a function of RTA temperature and time.

Figure 5c shows the linear correlation of graphene thickness with the RTA time at all temperature ranges and the increase of RTA temperature and time results in the increase of thickness of the resulting layers. Since the solubility of carbon in nickel is temperature-dependent,[44] carbon atoms precipitate as a graphene layer on the nickel surface, with the rest remaining in the nickel film. However, we note that the resulting films have a limited thickness (<2 nm), even for an extended RTA time, possibly because of the limited amount of unintentionally introduced carbon sources on the Ni surface, and this is one of the advantages in this synthesis methodology, since we can reproducibly obtain very thin graphene layers using the Ni films without the need for complex processing conditions, in contrast to the CVD method.

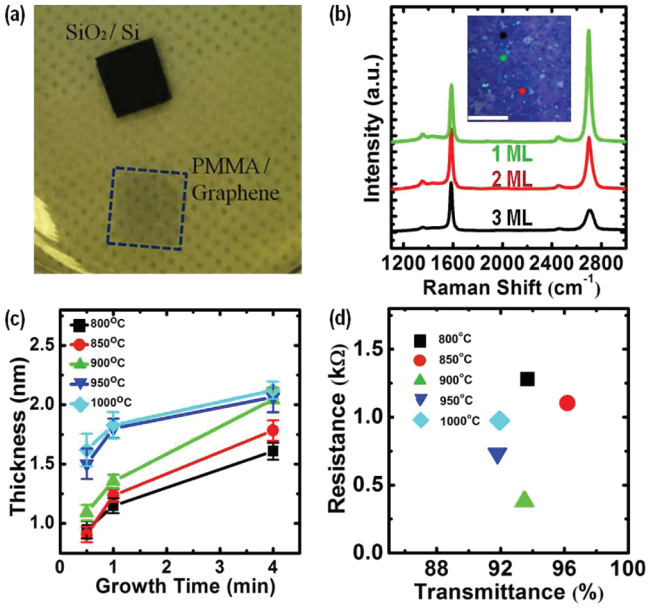

Figure 5. (a) Photograph of a floating PMMA/graphene film released from a Ni surface by etching in a $FeCl_3$ solution to transfer to other substrates for further evaluation. (b) Representative optical microscopy image of transferred graphene film on a SiO_2/Si substrate and Raman spectra from green, red, and black spots, showing the presence of one, two, and three layers of graphene, respectively. The scale bar in the inset is 20 μm. (c) The heights of graphene films upon transfer to SiO_2/Si substrates after RTA growth as a function of RTA temperature and time. (d) Sheet resistances and transmittances of graphene films grown at a temperature range of 800−1000 °C for 4 min then transferred to SiO_2/Si and quartz substrates, respectively.

3.5. Optoelectronic Characterization of Graphene. In the case of the graphene layers transferred onto quartz substrates, we obtain ~91%−97% transmittance (Figure 5d). These samples were obtained after the RTA process at temperatures in the range of 800−1000 °C for 4 min under vacuum. Considering 2.3% absorption of incident white light in an individual graphene layer,[45] it can be inferred that these films are 2−4 layer thick, which is in good agreement with the AFM data of the graphene layers on a SiO_2 surface. The sheet resistances of the graphene layers are ~380−1280 Ω/sq, as measured by the TLM method.[31−33] This demonstrates the potential to simply grow useful graphene layers with a controllable thickness over large areas.

4. CONCLUSIONS

In conclusion, we show that few-layer graphene with a controllable thickness can be simply grown by annealing the nickel films at high temperatures under vacuum. These layers demonstrate comparable structural and optoelectronic qualities to existing graphene materials grown on a nickel surface by the chemical vapor deposition (CVD) method but are synthesized without the need for complex processing conditions. This process is highly reproducible, and the thickness of the graphene layers is controlled by the RTA temperature and time. This simple and potentially inexpensive method of synthesizing novel 2D carbon films offers a wide choice of graphene films for possible electronic and optoelectronic applications, where graphene materials are needed in large quantities.

AUTHOR INFORMATION

Corresponding Author

*Tel.: +82-52-217-2312. Fax: +82-52-217-2309. E-mail address: sykwon@unist.ac.kr.

Notes

The authors declare no competing financial interest.

ACKNOWLEDGMENTS

We gratefully acknowledge support from the Basic Science Research Program through the National Research Foundation (NRF) of Korea funded by the Ministry of Education, Science and Technology (Grants No. 2010-0009824, 2010-0004370, 2011-0029212, and 2011-0014877) and from the Human Resources Development Program through the Korea Institute of Energy Technology Evaluation and Planning (KETEP) grant funded by the Korea Government Ministry of Knowledge Economy (Grant No. 20114030200010). This work has benefited from the use of the facilities at UNIST Central Research Facilities.

REFERENCES

(1) Novoselov, K. S.; Geim, A. K.; Morozov, S. V.; Jiang, D.; Zhang, Y.; Dubonos, S. V.; Grigorieva, I. V.; Firsov, A. A. *Science* **2004**, *306*, 666−669.
(2) Novoselov, K. S.; Geim, A. K.; Morozov, S. V.; Jiang, D.; Katsnelson, M. I.; Grigorieva, I. V.; Dubonos, S. V.; Firsov, A. A. *Nature* **2005**, *438*, 197−200.
(3) Zhang, Y. B.; Tan, Y. W.; Stormer, H. L.; Kim, P. *Nature* **2005**, *438*, 201−204.
(4) Bolotin, K. I.; Sikes, K. J.; Jiang, Z.; Klima, M.; Fudenberg, G.; Hone, J.; Kim, P.; Stormer, H. L. *Solid State Commun.* **2008**, *146*, 351−355.
(5) Ohta, T.; Bostwick, A.; Seyller, T.; Horn, K.; Rotenberg, E. *Science* **2006**, *313*, 951−954.
(6) Son, Y. W.; Cohen, M. L.; Louie, S. G. *Phys. Rev. Lett.* **2006**, *97*, 216803.
(7) Balandin, A. A.; Ghosh, S.; Bao, W. Z.; Calizo, I.; Teweldebrhan, D.; Miao, F.; Lau, C. N. *Nano Lett.* **2008**, *8*, 902−907.
(8) Lee, C.; Wei, X. D.; Kysar, J. W.; Hone, J. *Science* **2008**, *321*, 385−388.
(9) Li, X. L.; Wang, X. R.; Zhang, L.; Lee, S. W.; Dai, H. J. *Science* **2008**, *319*, 1229−1232.
(10) Hao, L.; Qian, W.; Zhang, L.; Hou, Y. *Chem. Commun.* **2008**, 6576−6578.
(11) Qian, W.; Hao, R.; Hou, Y.; Tian, Y.; Shen, C.; Gao, H.; Liang, X. *Nano Res.* **2009**, *2*, 706−712.
(12) Cui, X.; Zhang, C.; Hao, R.; Hou, Y. *Nanoscale* **2011**, *3*, 2118−2126.
(13) Qian, W.; Cui, X.; Hao, R.; Hou, Y.; Zhang, Z. *ACS Appl. Mater. Interfaces* **2011**, *3*, 2259−2264.
(14) Berger, C.; Song, Z. M.; Li, X. B.; Wu, X. S.; Brown, N.; Naud, C.; Mayou, D.; Li, T.; Hass, J.; Marchenkov, A. N.; Conrad, E. H.; First, P. N.; de Heer, W. A. *Science* **2006**, *312*, 1191−1196.
(15) Brar, V. W.; Zhang, Y.; Yayon, Y.; Ohta, T.; McChesney, J. L.; Bostwick, A.; Rotenberg, E.; Horn, K.; Crommie, M. F. *Appl. Phys. Lett.* **2007**, *91*, 122102.
(16) Land, T. A.; Michely, T.; Behm, R. J.; Hemminger, J. C.; Comsa, G. *Surf. Sci.* **1992**, *264*, 261−270.
(17) Sutter, P. W.; Flege, J. I.; Sutter, E. A. *Nat. Mater.* **2008**, *7*, 406−411.
(18) Kwon, S.-Y.; Ciobanu, C. V.; Petrova, V.; Shenoy, V. B.; Bareno, J.; Gambin, V.; Petrov, I.; Kodambaka, S. *Nano Lett.* **2009**, *9*, 3985−3990.
(19) Reina, A.; Jia, X. T.; Ho, J.; Nezich, D.; Son, H. B.; Bulovic, V.; Dresselhaus, M. S.; Kong, J. *Nano Lett.* **2009**, *9*, 30−35.

(20) Kim, K. S.; Zhao, Y.; Jang, H.; Lee, S. Y.; Kim, J. M.; Ahn, J. H.; Kim, P.; Choi, J.-Y.; Hong, B. H. *Nature* **2009**, *457*, 706−710.
(21) Li, X. S.; Cai, W. W.; An, J. H.; Kim, S.; Nah, J.; Yang, D.; Piner, R.; Velamakanni, A.; Jung, I.; Tutuc, E.; Banerjee, S. K.; Colombo, L.; Rouff, R. S. *Science* **2009**, *324*, 1312−1314.
(22) Dai, B.; Fu, L.; Zou, Z.; Wang, M.; Xu, H.; Wang, S.; Liu, Z. *Nat. Commun.* **2011**, *2*, 522.
(23) Gao, L.; Ren, W.; Xu, H.; Jin, L.; Wang, Z.; Ma, T.; Ma, L.-P.; Zhang, Z.; Fu, Q.; Peng, L.-M.; Bao, X.; Cheng, H.-M. *Nat. Commun.* **2012**, *3*, 699.
(24) Bae, S.; Kim, H.; Lee, Y.; Xu, X. F.; Park, J. S.; Zheng, Y.; Balakrishnan, J.; Lei, T.; Kim, H. R.; Song, Y. I.; Kim, Y.-J.; Kim, K. S.; Ozyilmaz, B.; Ahn, J.-H.; Hong, B. H.; Iijima, S. *Nat. Nanotechnol.* **2010**, *5*, 574−578.
(25) Sun, Z.; Yan, Z.; Yao, J.; Beitler, E.; Zhu, Y.; Tour, J. M. *Nature* **2010**, *468*, 549−552.
(26) Zheng, M.; Takei, K.; Hsia, B.; Fang, H.; Zhang, X. B.; Ferralis, N.; Ko, H.; Chueh, Y.-L.; Zhang, Y.; Maboudian, R.; Javey, A. *Appl. Phys. Lett.* **2010**, *96*, 063110.
(27) Zhang, H.; Feng, P. X. *Carbon* **2010**, *48*, 359−364.
(28) García, J. M.; He, R.; Jiang, M. P.; Kim, P.; Pfeiffer, L. N.; Pinczuk, A. *Carbon* **2011**, *49*, 1006−1012.
(29) Pollard, A. J.; Nair, R. R.; Sabki, S. N.; Staddon, C. R.; Perdigao, L. M. A.; Hsu, C. H.; Garfitt, J. M.; Gangopadhyay, S.; Gleeson, H. F.; Geim, A. K.; Beton, P. H. *J. Phys. Chem. C* **2009**, *113*, 16565−16567.
(30) Casiraghi, C.; Pisana, S.; Novoselov, K. S.; Geim, A. K.; Ferrari, A. C. *Appl. Phys. Lett.* **2007**, *91*, 233108.
(31) Reeves, G. K.; Harrison, H. B. *IEEE Electron Device Lett.* **1982**, *3*, 111−113.
(32) Xia, F.; Perebeinos, V.; Lin, Y.; Wu, Y.; Avouris, P. *Nat. Nanotechnol.* **2011**, *6*, 179−184.
(33) Kwak, J.; Chu, J. H.; Choi, J.-K.; Park, S.-D.; Go, H.; Kim, S. Y.; Park, K.; Kim, S.-D.; Kim, Y.-W.; Yoon, E.; Kodambaka, S.; Kwon, S.-Y. *Nat. Commun.* **2012**, *3*, 645.
(34) McIntyre, N. S.; Chan, T. C.; Chen, C. *Oxid. Met.* **1990**, *33*, 457−479.
(35) Klein, J. C.; Hercules, D. M. *J. Catal.* **1983**, *82*, 424−441.
(36) Kraus, L. S.; Pines, H.; Butt, J. B. *J. Catal.* **1991**, *128*, 337−351.
(37) Czekaj, I.; Loviat, F.; Raimondi, F.; Wambach, J.; Biollaz, S.; Wokaun, A. *Appl. Catal., A* **2007**, *329*, 68−78.
(38) Desimoni, E.; Casella, G. I.; Salvi, A. M. *Carbon* **1992**, *30*, 521−526.
(39) Sinharoy, S.; Levenson, L. L. *Thin Solid Films* **1978**, *53*, 31−36.
(40) Archer, D. G. *J. Phys. Chem. Ref. Data* **1999**, *28*, 1485−1507.
(41) Wallner, H.; Preis, W.; Gamsjäger, H. *Thermochim. Acta* **2002**, *382*, 289−296.
(42) Langmuir, I. *Phys. Rev. (Series I)* **1912**, *43*, 401−422.
(43) Fonda, G. R. *Phys. Rev.* **1928**, *31*, 260−266.
(44) Shelton, J. C.; Patil, H. R.; Blakely, J. M. *Surf. Sci.* **1974**, *43*, 493−520.
(45) Nair, R. R.; Blake, P.; Grigorenko, A. N.; Novoselov, K. S.; Booth, T. J.; Stauber, T.; Peres, N. M. R.; Geim, A. K. *Science* **2008**, *320*, 1308.